

Breakup coupling Effects on Near-Barrier ${}^6\text{Li}$, ${}^7\text{Be}$ and ${}^8\text{B} + {}^{58}\text{Ni}$ Elastic Scattering Compared

N. Keeley, R.S. Mackintosh, C. Beck

► **To cite this version:**

N. Keeley, R.S. Mackintosh, C. Beck. Breakup coupling Effects on Near-Barrier ${}^6\text{Li}$, ${}^7\text{Be}$ and ${}^8\text{B} + {}^{58}\text{Ni}$ Elastic Scattering Compared. 10th International Conference on Nucleus-Nucleus Collisions, Aug 2009, Beijing, China. in2p3-00438250

HAL Id: in2p3-00438250

<http://hal.in2p3.fr/in2p3-00438250>

Submitted on 3 Dec 2009

HAL is a multi-disciplinary open access archive for the deposit and dissemination of scientific research documents, whether they are published or not. The documents may come from teaching and research institutions in France or abroad, or from public or private research centers.

L'archive ouverte pluridisciplinaire **HAL**, est destinée au dépôt et à la diffusion de documents scientifiques de niveau recherche, publiés ou non, émanant des établissements d'enseignement et de recherche français ou étrangers, des laboratoires publics ou privés.

Breakup Coupling Effects on Near-Barrier ${}^6\text{Li}$, ${}^7\text{Be}$ and ${}^8\text{B} + {}^{58}\text{Ni}$ Elastic Scattering Compared

N. Keeley^a, R.S. Mackintosh^b and C. Beck^c

^aDepartment of Nuclear Reactions, The Andrzej Sołtan Institute for Nuclear Studies, ul. Hoża 69, 00-681 Warsaw, Poland

^bDepartment of Physics and Astronomy, The Open University, Milton Keynes, MK7 6AA, United Kingdom

^cInstitut Pluridisciplinaire Hubert Curien et Université Louis Pasteur, Boîte Postale 28, F-67037 Strasbourg Cedex 2, France

New data for near-barrier ${}^6\text{Li}$, ${}^7\text{Be}$ and ${}^8\text{B} + {}^{58}\text{Ni}$ elastic scattering enable a comparison of breakup coupling effects for these loosely-bound projectiles. Coupled Discretised Continuum Channels (CDCC) calculations suggest that the large total reaction cross sections for ${}^8\text{B} + {}^{58}\text{Ni}$ are dominated by breakup at near-barrier energies, unlike ${}^6\text{Li}$ and ${}^7\text{Be}$ where breakup makes a small contribution. In spite of this, the CDCC calculations show a small coupling influence due to breakup for ${}^8\text{B}$, in contrast to the situation for ${}^6\text{Li}$ and ${}^7\text{Be}$. An examination of the S matrices gives a clue to this counter-intuitive behaviour.

1. INTRODUCTION

Recent data [1] for near-barrier ${}^6\text{Li}$, ${}^7\text{Be}$ and ${}^8\text{B} + {}^{58}\text{Ni}$ elastic scattering allow some interesting comparisons for these weakly-bound nuclei. Optical model fits find much larger total reaction cross sections (σ_{R}) for ${}^8\text{B}$ than for ${}^6\text{Li}$ or ${}^7\text{Be}$, even when “reduced” [2]; while the reduced σ_{R} for other weakly-bound projectiles lie on a universal curve, those for ${}^8\text{B}$ and ${}^6\text{He}$ are significantly larger [1]. The low ${}^8\text{B} \rightarrow {}^7\text{Be} + p$ breakup threshold (0.1375 MeV) suggests a dominant contribution to the direct part of σ_{R} . This is not automatic: for ${}^6\text{He}$ with an $\alpha + 2n$ breakup threshold of 0.973 MeV, $1n$ - and $2n$ -stripping are the main contributors to σ_{R} at near-barrier energies. However, the weakly-bound proton in ${}^8\text{B}$ experiences Coulomb barrier and charge polarisation effects tending to suppress transfer.

CDCC calculations [3] find that breakup does dominate the direct component of σ_{R} for ${}^8\text{B}$: as the cross sections are large — of the order of 100 mb or more — one might expect an equally important coupling effect on the elastic scattering angular distribution. However, this is not the case [3]. We thus have an apparent paradox: ${}^6\text{Li}$, with a relatively small breakup cross section, exhibits an important breakup coupling effect on the elastic scattering (see e.g. [4]) whereas ${}^8\text{B}$, with a large breakup cross section, shows only a modest coupling effect. A comparison of S matrices obtained from CDCC calculations for ${}^6\text{Li}$, ${}^7\text{Be}$ and ${}^8\text{B} + {}^{58}\text{Ni}$ provides a clue to this behaviour. Preliminary dynamic polarisation potentials (DPPs) are also presented.

2. CALCULATIONS

Calculations were performed with the code FRESKO [5]: only a brief outline is given here. The ${}^6\text{Li}$, ${}^7\text{Be}$ and ${}^8\text{B}$ nuclei were modelled as $\alpha + d$, $\alpha + {}^3\text{He}$ and ${}^7\text{Be} + p$ clusters, respectively. The ${}^7\text{Be}$ core was treated as inert but its non-zero spin was retained. Interaction potentials were obtained by Watanabe-type folding of global optical potentials, with a ${}^6\text{Li}$ potential as surrogate for ${}^7\text{Be}$, the well-depths being adjusted to give the best fit to the data. The ${}^6\text{Li}$ and ${}^7\text{Be}$ calculations were similar to those in [4] and [6], but with finer continuum binning for ${}^7\text{Be}$. The ${}^8\text{B}$ calculations included couplings to the $L = 0, 1, 2$ and 3 continuum and the 0.774 MeV 1^+ and 2.32 MeV 3^+ resonances. Good fits to all the data were obtained. Due to lack of space we show only results for the same values of $E_{\text{c.m.}} - V_{\text{B}}$ for each system, where V_{B} is the nominal Coulomb barrier, taking as our ‘‘benchmark’’ the ${}^8\text{B}$ data at $E_{\text{lab}} = 29.26$ MeV. This procedure yields values of $E_{\text{lab}} = 19.04$ and 24.12 MeV for ${}^6\text{Li}$ and ${}^7\text{Be} + {}^{58}\text{Ni}$, respectively. In this way effects due to differences in projectile charge should be minimised.

Results are presented in Fig. 1: the coupling effect is much stronger for ${}^6\text{Li}$ and ${}^7\text{Be}$, with ${}^6\text{Li} \rightarrow \alpha + d$ and ${}^7\text{Be} \rightarrow \alpha + {}^3\text{He}$ breakup thresholds of 1.47 and 1.59 MeV, respectively, an order of magnitude larger than the ${}^8\text{B} \rightarrow {}^7\text{Be} + p$ threshold. The ${}^6\text{Li} \rightarrow \alpha + d$ process

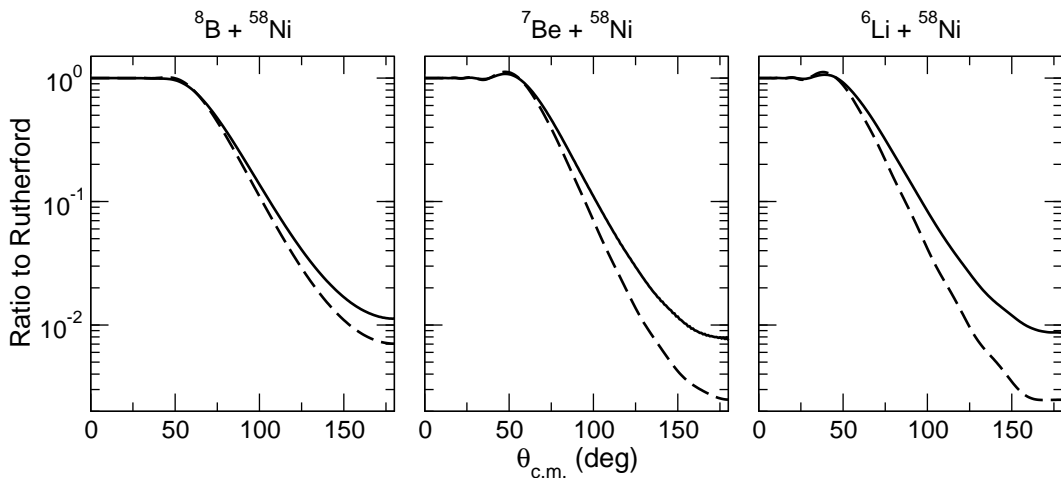


Figure 1. CDCC calculations for ${}^8\text{B}$, ${}^7\text{Be}$ and ${}^6\text{Li} + {}^{58}\text{Ni}$ at $E_{\text{lab}} = 29.26, 24.12$ and 19.04 MeV. Solid and dashed curves denote full and no-coupling results, respectively.

has the additional peculiarity that it cannot proceed via dipole breakup. If we include population of the bound $1/2^-$ state in ${}^7\text{Be}$ (considering breakup as an inelastic excitation) the total breakup cross sections for both ${}^6\text{Li}$ and ${}^7\text{Be}$ are about a factor of three smaller than for ${}^8\text{B}$. To obtain a clue to this apparent paradox, we show in Fig. 2 the modulus and argument of the J -weighted S matrices [7] obtained from full and no-coupling calculations. The coupling effect on $|S|$ is almost negligible for ${}^8\text{B}$ and largest for ${}^6\text{Li}$, but qualitatively

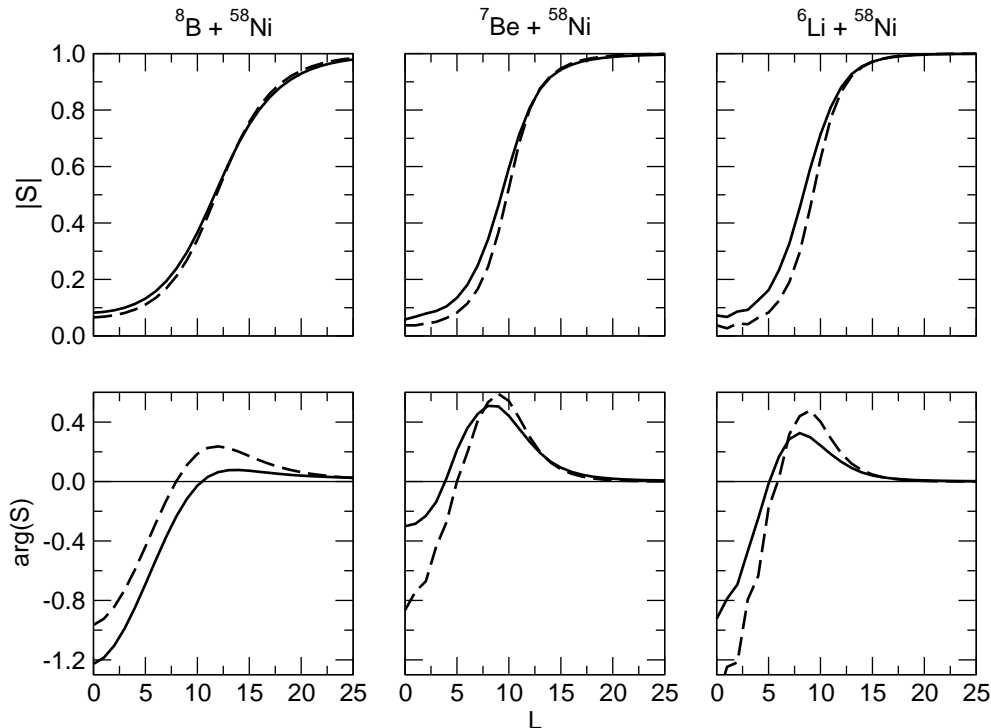


Figure 2. $|S|$ and $\arg(S)$ from CDCC calculations for ${}^8\text{B}$, ${}^7\text{Be}$ and ${}^6\text{Li} + {}^{58}\text{Ni}$ at $E_{\text{lab}} = 29.26, 24.12$ and 19.04 MeV. Solid and dashed curves denote full and no-coupling results, respectively.

similar for all three nuclei: a decrease of $|S|$ at small L and an increase at large L . By contrast, for $\arg(S)$ the coupling effect is greatest for ${}^8\text{B}$, smallest for ${}^7\text{Be}$ and intermediate for ${}^6\text{Li}$.

3. DISCUSSION

For protons and other light particles, changes in $|S|$ correspond to changes in the imaginary part of the potential, while changes in $\arg(S)$ correspond to changes in the real part. While this simple picture is not so clear-cut in the presence of strong absorption (as here) it provides a useful guide. Thus, the coupling effect on $|S|$ suggests *reduced* absorption at small L , switching to increased absorption at large L . The effect on $\arg(S)$ suggests repulsion at small L and attraction at large L . These effects are qualitatively similar for all three nuclei. The fact that the coupling effect on both the elastic scattering and $|S|$ is so small for ${}^8\text{B}$ suggests that, paradoxical as it may seem for a coupling producing such a large cross section, its effective imaginary potential is small.

DPPs may be obtained by inversion of the S matrix, see e.g. [8]. In Fig. 3 we show the results of such a procedure for ${}^8\text{B}$ and ${}^7\text{Be}$. Those for ${}^7\text{Be}$ are preliminary; we expect the final DPPs to be somewhat smoother. While the DPPs are qualitatively similar,

short-range repulsion and long-range attraction combined with surface absorption (this behaviour seems to be universal, see e.g. [9]), the details are very different. The small

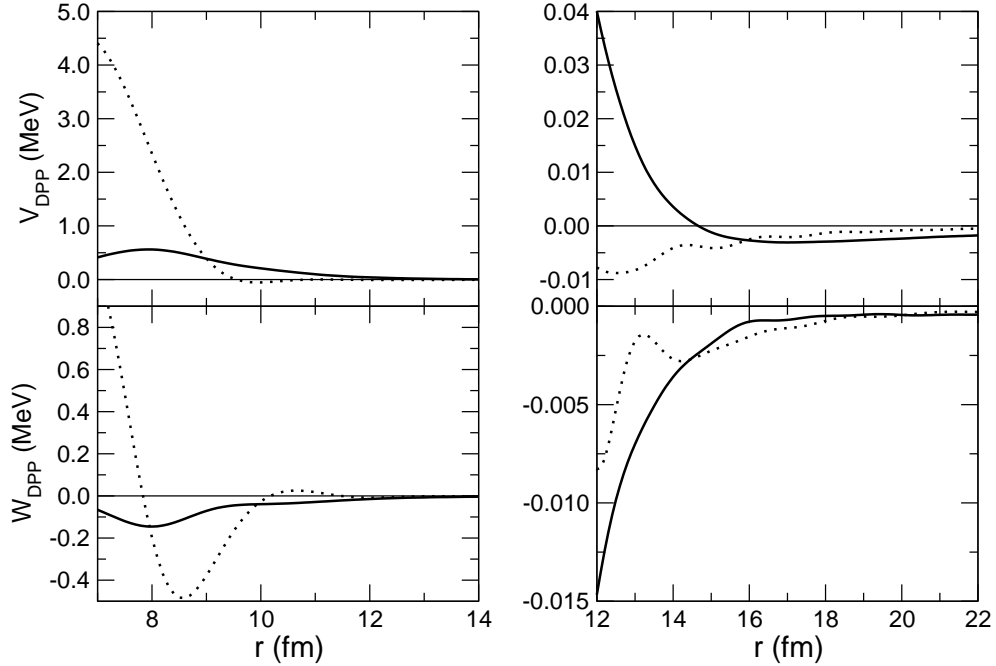


Figure 3. DPPs from CDCC calculations for ${}^8\text{B}$ (solid curves) and ${}^7\text{Be}$ (dotted curves).

imaginary DPP for ${}^8\text{B}$ is particularly striking, confirming the conclusions inferred from the S matrices. The surface repulsion for ${}^8\text{B}$ is also much smaller than for ${}^7\text{Be}$, although for radii larger than about 9 fm it is significantly larger than for ${}^7\text{Be}$, having a longer, more repulsive tail. Our results show that a large cross section is no guarantee of a large coupling effect. The S matrices and DPPs shed some light on this, but it remains to be explained at a more fundamental level.

REFERENCES

1. E.F. Aguilera et al., Phys. Rev. C 79 (2009) 021601(R).
2. P.R.S. Gomes et al., Phys. Rev. C 71 (2005) 017601.
3. J. Lubian et al., Phys. Rev. C 79 (2009) 064605.
4. C. Beck, N. Keeley and A Diaz-Torres, Phys. Rev. C 75 (2007) 054605.
5. I.J. Thompson, Comput. Phys. Rep. 7 (1988) 167.
6. N. Keeley, K.W. Kemper and K. Rusek, Phys. Rev. C 66 (2002) 044605.
7. N. Keeley and R.S. Mackintosh, Phys. Rev. C 77 (2008) 054603.
8. V.I. Kukulin and R.S. Mackintosh, J. Phys. G 30 (2004) R1.
9. K. Rusek, Eur. Phys. J. A (2009), doi: 10.1140/epja/i2009-10838-x.